



Comprehensive machinability assessment of Ti6Al4V alloy during drilling and helical milling using sustainable dry condition

Anupama Hiremath¹ · Rashmi L. Malghan² · Gururaj Bolar¹ · Ashwin Polishetty³

Received: 30 January 2024 / Accepted: 18 June 2024
© The Author(s) 2024

Abstract

Cutting fluids are an essential requirement while machining materials like Ti6Al4V alloy exhibiting low thermal conductivity and work hardening behavior. However, the non-biodegradable nature of the oil increases carbon emissions and causes serious health concerns, thus jeopardizing sustainability. In addition, complexity increases when drilling Ti6Al4V alloy due to the temperature build-up, leading to material adhesion and accelerated tool wear. The study, therefore, investigates the utility of helical milling for creating holes in Ti6Al4V alloy. The hole-making operations were appraised considering the chip morphology, microhardness, machining temperature, tool wear, and surface roughness. The findings show that hole-making using helical milling was beneficial since it produced lower thrust force. Measured temperatures during helical milling were significantly lower than in drilling. Helically milled holes displayed superior quality holes with lower surface roughness; however, at higher productivity conditions, chatter marks were noted. The microhardness was lower near the machined surface in the case of conventional drilling, indicating material softening. In comparison, helical milled holes displayed higher microhardness very close to the edge of the hole due to work hardening. The helical milling operation produced short discontinuous chips, which are desirable while machining Ti6Al4V alloy. Furthermore, the examination of the cutting tool showed material adhesion. The severity of tool damage was significantly lower during the helical milling operation. The initial assessment indicates that helical milling is an adept process for making holes in Ti6Al4V alloy.

Keywords Sustainable machining · Drilling · Helical milling · Thrust force · Surface roughness · Microhardness

1 Introduction

Due to growing concerns about environmental degradation, adhering to sustainable practices in almost all engineering applications is imperative. This calls for the judicious selection of both materials and methods that are environmentally friendly. Titanium and its alloys are a class of light alloys

that are considered eco-friendly due to their inertness and recyclable capability. Titanium alloys possess an array of attractive properties, including impressive strength-to-weight ratio, low modulus, and formidable compressive strength at both high and cryogenic temperatures coupled with non-toxicity and resistance to corrosion [1, 2]. This has enabled titanium alloys to be used in aerospace, military, maritime, and biomedical applications [3, 4].

However, titanium alloy machining is often challenging considering their high melting point, low thermal conductivity, low elastic modulus, and very poor chip evacuation characteristics [5, 6]. Titanium alloys are prone to sub-surface damage resulting from the extreme heat build-up at the cutting zones on account of their poor conductivity [7, 8]. This situation also leads to accelerated tool wear, making dry machining of titanium alloys very uneconomical and, simultaneously, not feasible [9]. Thus, conventional machining of titanium alloys heavily relies upon flooding the cutting zone with coolants that carry away the excess heat generated at

✉ Gururaj Bolar
gururaj.bolar@manipal.edu

¹ Department of Mechanical and Industrial Engineering, Manipal Institute of Technology, Manipal Academy of Higher Education, Manipal 576104, India

² Department of Data Science and Computer Applications, Manipal Institute of Technology, Manipal Academy of Higher Education, Manipal 576104, India

³ School of Engineering, Computer and Mathematical Science, Auckland University of Technology, Auckland 1010, New Zealand

the cutting zones coupled with lubricants that minimize the interfacial [10, 11]. The requirement of such coolants, lubricants, and cutting fluids for commercial machining of titanium alloys is so high that they account for approximately 17% of the total cost of the manufactured component compared to only 4% of the total cutting tool costs [12]. These cutting fluids are made up of a combination of hazardous chemicals to humans and the environment [13]. In fact, it is reported that cutting fluids accounts for 80% of skin-related occupational hazards [14]. In view of this, there is a need to develop and apply sustainable machining practices that utilize nil to negligible quantities of such cutting fluids. With the advent of carbide and ceramic based tools, dry machining has emerged as a promising sustainable alternative to coolant-based machining operations [15].

Conventional dry drilling, which is often carried out during the concluding stages of the production process, is used to produce holes in structural components to facilitate mechanical bolting to fasten all the components and assemble the final structure [16]. It has been reported that drilling accounts for nearly 40–60% of all the machining processes employed [17]. However, it is to be noted that, during conventional drilling of the titanium alloy, heat dissipation is often challenging and cumbersome. The drill tool is constrained within the hole being drilled, and the chips of titanium alloy do not carry away much of the heat owing to the low thermal conductivity of Ti6Al4V. Heat entrapment is detrimental to tool life and hole surface quality [18]. Also, to have holes with superior finish, it is desirable to select higher levels of cutting speed and feed rates during drilling. These factors, along with poor thermal conductivity of Ti6Al4V, contribute to escalating cutting zone temperature. Coelho et al. [19] found that the drilling tool temperature is directly proportional to the cutting speed and feed rates. Further, they reported a 56.9% increase in the tool temperature at higher feed rates. Zhang et al. [20] highlighted that for drilling titanium alloy, the tool life drastically reduces with dry cutting due to higher temperatures as the cutting speed increases. When drilling with 73.2 m/min cutting speed and feed of 0.025 mm/tooth feed, a peak cutting temperature of approximately 1060 °C was registered [21]. Even with minimal quantity lubrication (MQL) implementation, the drilling temperature fluctuated between 590 and 640 °C, even at relatively low speeds of 35 m/min. This fluctuation in drilling temperature initiated the tool wear, consequently reducing the tool's operational lifespan [22]. In titanium alloy machining, lower speeds and feeds are desirable to mitigate the detrimental impact of elevated cutting temperatures on tool longevity. While these reduced cutting speeds and feeds are effective in minimizing both cutting temperature and tool wear, they do come at a cost - they inevitably impede material removal rates and can escalate the expenses

associated with machining titanium alloys. In conventional drilling of titanium alloys, the escalated cutting temperatures reduce the surface quality and impair the tool life [23]. Elevated cutting temperatures, leading to excessive plastic deformation, can give rise to microcracks and induce tensile residual stresses [24]. Furthermore, there have been documented cases of an undesirable heat-affected zone (HAZ) forming at these heightened cutting temperatures [25]. As the cutting temperature increases, so does the surface roughness. Such an escalation is attributed to molten chips adhering to the bore surface, raising the surface roughness [26].

Though conventional dry drilling is sustainable, several challenges concerning tool life and surface integrity prevail. The process of mitigating the adverse effects of cutting temperature by lowering the cutting speed has, in turn, been proven to reduce the process efficiency. Recognizing the challenges inherent in drilling titanium alloys, researchers have delved into alternative hole-making technologies to mitigate tool expenses while enhancing product quality and productivity and keeping sustainability in view. One such sustainable method under exploration is the helical milling process [27]. This process has shown promise in reducing the cutting forces exerted during hole processing compared to conventional drilling methods, even when dealing with materials like titanium alloys [28]. According to Wang et al. [29], axial force diminished by 90% with helical milling as against conventional drilling. Iqbal et al. [30] reported that helical milling of Ti-6Al-4 V is sustainable, and using micro-lubricants and a larger helix angle is beneficial, as it reduces the process cost and lowers the tool wear. Moreover, dry milling of Ti6Al4V alloy resulted in a very small HAZ as the highest recorded machining temperature was approximately 235 °C when the speed and feed were maintained at 60 m/min and 0.6 mm/revolution, respectively. Further, helical milling can effectively produce holes in Ti6Al4V alloy at cutting speeds as low as 20 m/min and a lower feed of 0.2 mm/revolution [31]. Recent exploration of vibration-assisted helical milling of Ti6Al4V showed that the process helped lower the transverse force and thrust force by 38.1% and 13.9%, respectively, and improved the surface finish [32].

From the published literature, it is visible the hole drilling in Ti6Al4V alloy is a challenging task. Excessive cutting load and temperatures can affect the surface integrity and tool life. Moreover, size of the chips produced in drilling is an issue since it influences the hole surface quality. However, helical milling demonstrated superior performance under comparable process parameters with reduced cutting forces, smoother surface finishes, and lower machining temperatures. While dry helical milling shows promise, there is room for enhancing its productivity. Exploring hole processing with higher material removal rates using dry

helical milling remains uncharted territory. Furthermore, the implications of heightened productivity on surface quality, machining temperature, and tool longevity are unclear. Hence, the study explores the drilling and helical milling of Ti6Al4V, considering chip morphology, microhardness, surface roughness, tool wear, and machining temperature under sustainable dry-cutting conditions.

2 Materials and methods

The machining trials were performed on Ti6Al4V alloy workpiece. The workpiece was mounted on a 3-axis CNC machine tool setup (AMC Spark), using a setup shown in Fig. 1(a). Tungsten carbide drill of 6.8 mm diameter was used to conduct the drilling trials. Helical milling trials were executed with 5 mm diameter solid carbide end mill, as shown in Fig. 1(b).

Thrust force measurement was accomplished using a force dynamometer (*Kistler 9272*) and a charge amplifier (*Kistler 5070 A*) (see Fig. 2(a)). Cutting force data was acquired for 60 s at a sampling rate of 2000 Hz and further processed and analyzed using Dynoware software. The surface roughness data was obtained employing a perthometer (*Taylor Hobson – Form Talysurf 50*), as seen in Fig. 2(b). Stylus had a tip radius of 2.5 μm . Measurements were made considering 0.8 mm as sampling length and 4 mm evaluation length. The boreholes were sectioned axially to evaluate the surface and sub-surface microhardness. The section part was polished before the micro-hardness measurement using a digital micro-hardness tester (*OmniTech*), as seen in Fig. 2(c). An optical microscope (*Olympus - BX53M*) was used to capture the surface texture (see Fig. 2(d)). A scanning electron microscope (SEM) (*Carl Zeiss EVO MA18*) was utilized to characterize tool wear (Fig. 2(e)). An infrared (I.R.) camera (*Fluke Ti32*) was utilized to measure the machining temperature. The deployed camera has an accuracy of ± 2 $^{\circ}\text{C}$ and a measuring range of 20 $^{\circ}\text{C}$ to 600 $^{\circ}\text{C}$. For a uniform and accurate temperature measurement, the CARALL workpiece was covered using matte black paint, having a thermal emissivity of 0.95. The CARALL samples were rigidly fixed on the vertical machining center, while

the I.R. camera was placed 0.2 m away from the work material (see Fig. 2(f)).

The process performance is dependent on the selected process variables. However, limited published studies deal with the helical milling of Ti6Al4V alloy. Therefore, the experiments were planned based on the drilling process parameters, which are widely available in the literature. In order to carry out a meaningful investigation, parameters viz., cutting speed and feed rate for hole drilling operation were selected considering the published literature [17, 33, 34], cutting tool constraint, and material cost. Drilling speed and feed were set at three levels each, and nine experiments were executed accordingly. Each trial was repeated thrice, and average of response values was analyzed. Thereafter, process variables for helical milling operation were selected considering a parity in process productivity, such that the average machining times for both hole processing were similar. For the helical milling operation, axial feed and cutting speed were also varied at three levels while maintaining the tangential feed at 0.12 mm/tooth. Process variables for the two operations are listed in Table 1.

3 Results and discussion

3.1 Thrust force

Figure 3(a) displays the thrust force profile obtained for the hole drilled at a 50 m/min cutting speed and a feed of 0.06 mm/rev. As visualized, the profile can be split into three regions. In region-I (R-I), the force signal rises rapidly and reaches maximum (peak) when the drill chisel edge fully engages with the work specimen. The peak force observed as the chisel edge engages with the work specimen is attributed to the nature of cutting. Work material is parted-off by the blunt chisel edge, increasing the thrust load to maximum. Once the primary cutting edges fully engage with the work material, the force magnitude stabilizes and remains constant over region-II (R-II). In region-II, the material removal occurs by shearing action, thus lowering the force magnitude. Finally, in region-III (R-III), the force profile drops and reaches zero as the tool disengages and

Fig. 1 (a) Machining setup, (b) Cutting tools used

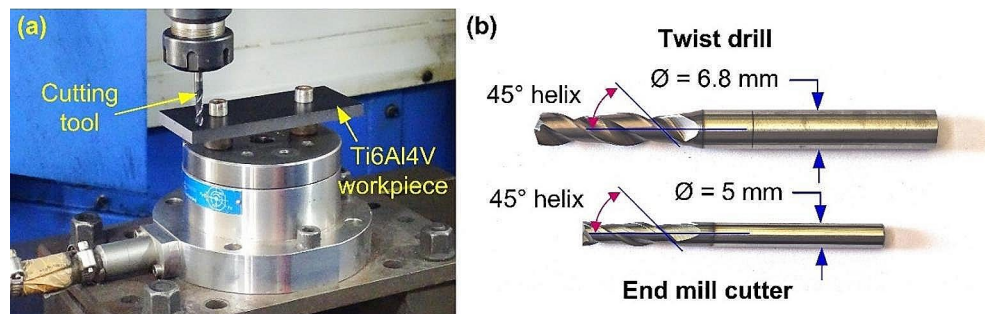


Fig. 2 Instruments utilized for various response measurements. Setup for measuring (a) Thrust force, (b) Surface roughness, (c) Microhardness, (d) Surface morphology, (e) Tool wear, (f) Machining temperature

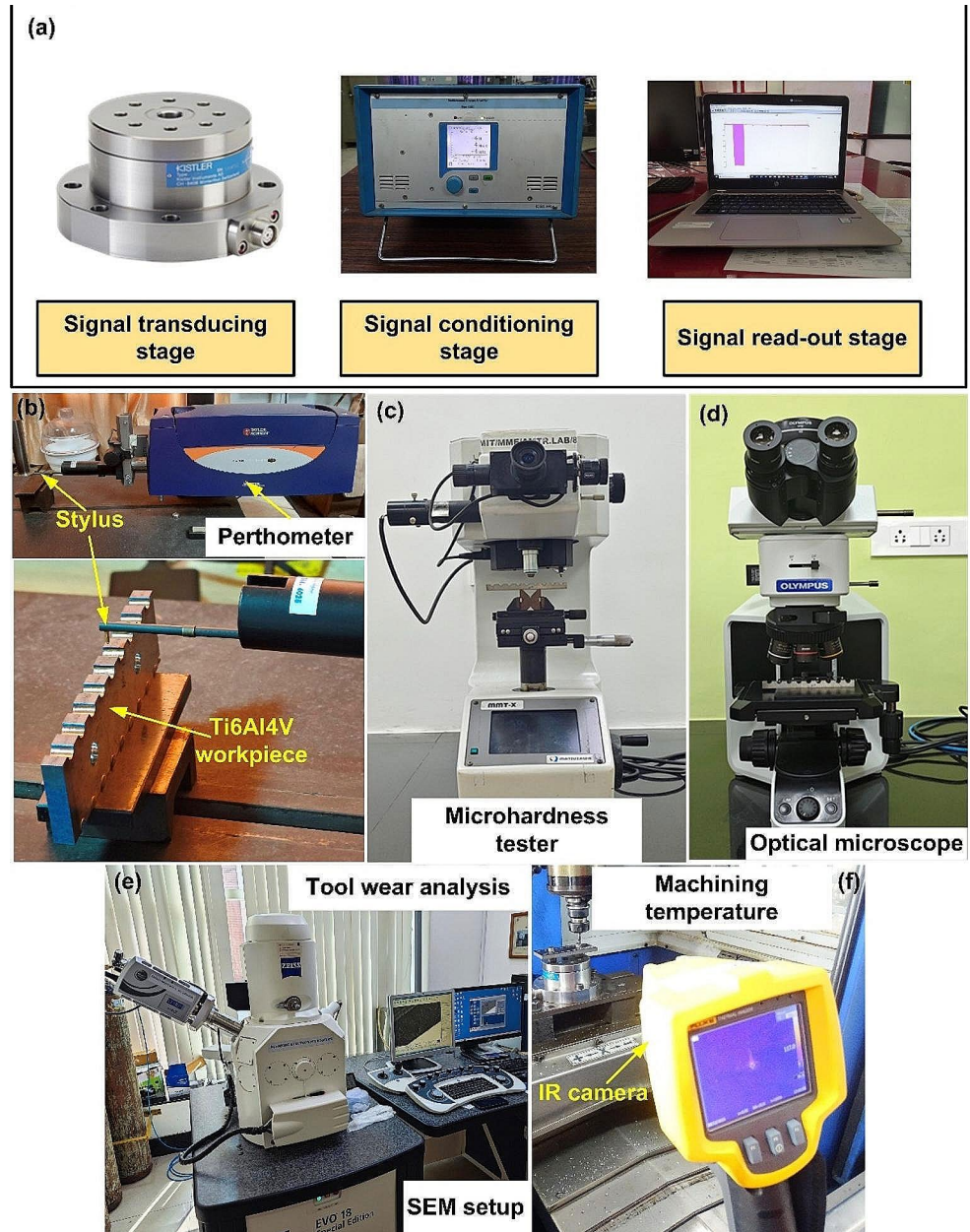


Table 1 Control parameters for machining trials and the machining time

Sl. No.	Cutting speed (m/min)	Axial feed (mm/rev)		Machining time (s)	
		Drilling	Milling	Drilling	Milling
1	25	0.02	0.2	61	62
2	50	0.02	0.2	38	39
3	75	0.02	0.2	30	29
4	25	0.04	0.4	38	38
5	50	0.04	0.4	26	25
6	75	0.04	0.4	22	22
7	25	0.06	0.6	30	31
8	50	0.06	0.6	22	22
9	75	0.06	0.6	20	21

fully exists from the work specimen. Contrary to the drilling operation, the thrust force for helical milling remains constant, as seen in Fig. 3(b). In region-I, the force profile increases and reaches maximum as the cutting commences at the frontal cutting edge. Over region-II, the force remains fairly constant, considering stable cutting by shearing action. As the end mill nears the hole exit, force magnitude drops and finally reaches zero, as indicated by region-III.

Furthermore, magnitude of drilling force is substantially higher than helical milling. For similar productivity conditions, an average thrust force of 435.2 N was recorded during drilling, while a force magnitude of 117.1 N was observed during helical milling, indicating a 73% decrease in the thrust force magnitude. In conventional drilling,

Fig. 3 Thrust force plots for (a) Drilling and (b) Helical milling

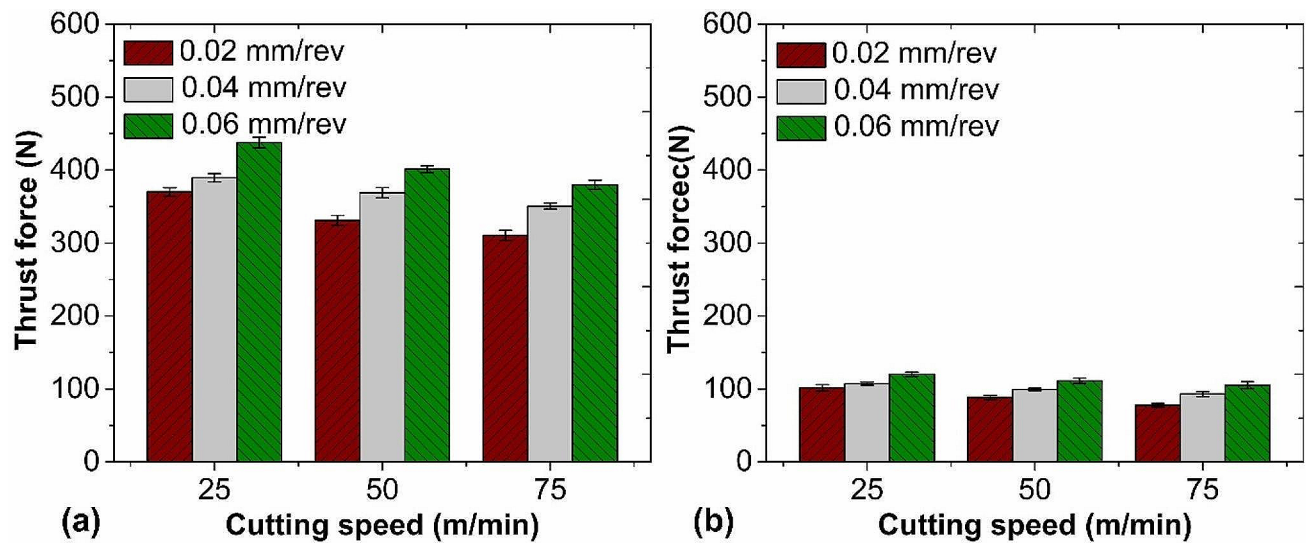
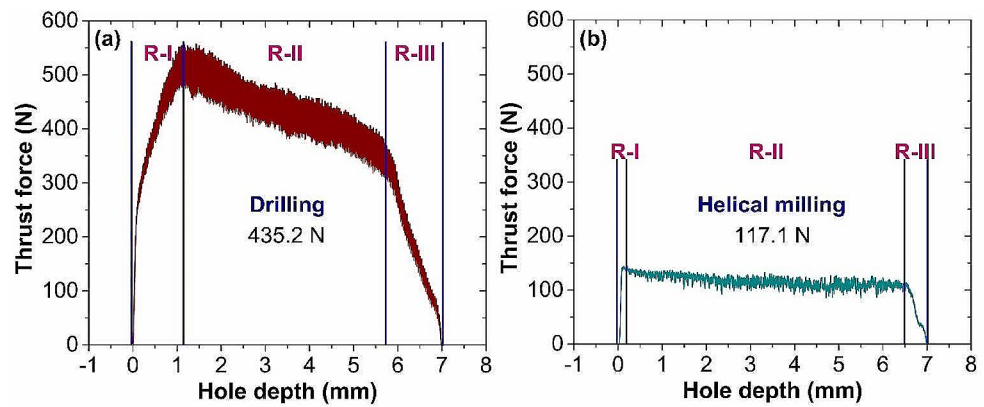


Fig. 4 Thrust force against process variables for (a) Drilling (b) Helical milling

material removal occurs at front cutting edges, which directs the force axially. Also, Ti6Al4V alloy exhibits severe work hardening tendency during machining, elevating the thrust force magnitude [27]. During helical milling, the material is sheared at axial and peripheral cutting edges, thus distributing the cutting load and lowering the thrust force [17].

Further, process variables and their impact on thrust force for both the hole-making operations were explored. Figure 4(a) indicates the behavior of thrust force at different cutting speeds. Thrust force dropped as the cutting speed increased. An average thrust force of 398.9 N was recorded when the cutting speed was maintained at 25 m/min. At a speed of 50 m/min, the thrust force increased to 367.1 N, while an average thrust force of 346.9 N was noted at 75 m/min. Similar observations were made during the helical milling process. At a speed of 25 m/min, an average thrust force of 109.6 N was registered. At a 50 m/min speed, the average measured thrust force was 99.4 N. When milling at 75 m/min, an average force of 91.8 N was recorded. Thrust force reduction with cutting speed is ascribed to

the material softening. The heat generation rate increases at higher speeds due to excessive plastic deformation [35]. The resulting increase in the cutting temperature softens the work material, easing the phenomenon of material shearing and reducing the thrust force.

The selection of axial feed also influenced the thrust force. For conventional drilling (see Fig. 4(a)), the average thrust force was 337.1 N, while feed was 0.02 mm/rev. At a feed of 0.04 mm/rev, the average force increased to 369.5 N. Further, an increase in the average force to 406.2 N was recorded while feed increased to 0.06 mm/rev. Figure 4(b) also depicts the deviation in average thrust force with axial feed during helical milling. Milling at 0.2 mm/rev, an average thrust force of 89.1 N was seen. As feed increased to 0.4 mm/rev, force increased to 99.7 N. When utilized axial feed was 0.6 mm/rev, magnitude of the thrust force was 112.1 N. Thrust force increased as axial feed increased for both hole-making operations. As the axial feed is increased, uncut chip thickness increases. As a result, the resistance to the material shearing also increases, thus increasing the

thrust force. However, out of the two hole-making operations, significantly lower forces were recorded for helical milling, exemplifying the usefulness of the process.

3.2 Surface roughness

Surface finish is an important requirement of functional parts in manufacturing processes. It is thus essential to evaluate the surface quality of holes processed during the two hole-making operations. In comparison to conventional drilling, magnitude of the surface roughness was significantly lower in helical milled holes (see Fig. 5). For similar productivity conditions (Exp No. 5), surface roughness of $1.21\ \mu\text{m}$ was measured in the drilled sample, while a surface roughness of $0.53\ \mu\text{m}$ was observed in the helical milled holes, indicating a 56% decrease in surface roughness. Holes subjected to drilling showcased higher roughness. Conventional drilling produces lengthy chips that are strain-hardened. These chips wind around the drill tool and scrape the hole surface. This leads to secondary cutting, generating deep ridges on the surface, thus increasing the surface roughness. The drill tool is also subjected to bending action due to the higher thrust load, resulting in unstable cutting with diminished surface finish [17].

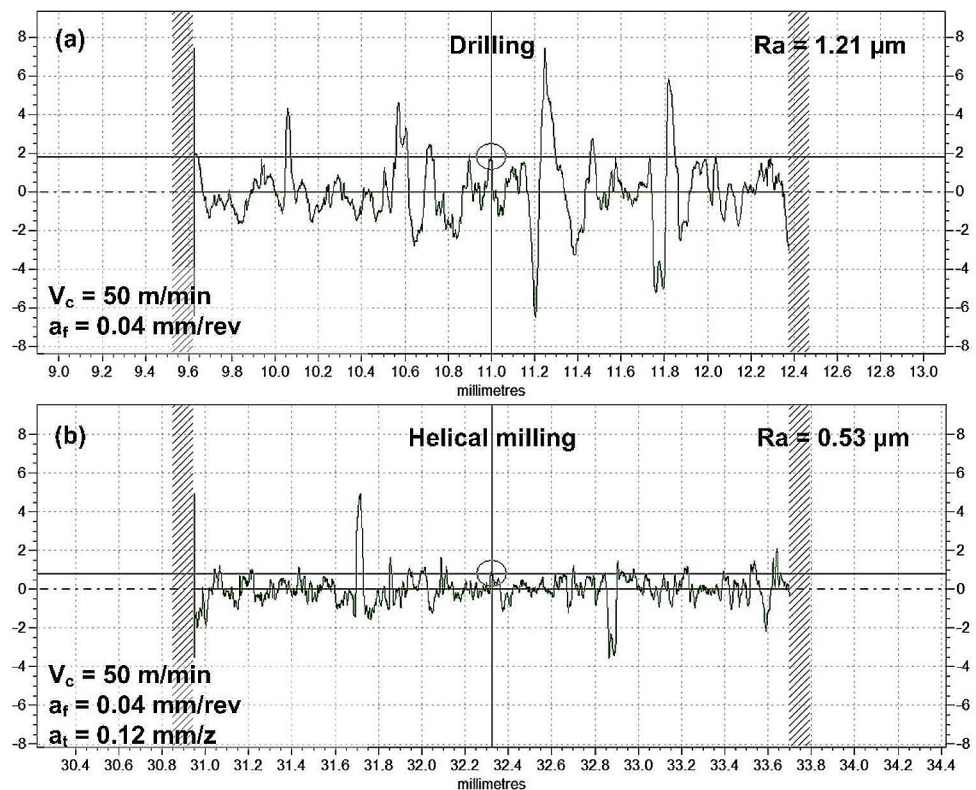
As compared to the drilled holes, helical milled holes exhibited lower surface roughness. The helical milling involves discontinuous cutting where a smaller diameter tool moves along a helical tool path and removes the material to

form a larger hole. In the process, material is removed as discontinuous chips, thereby lowering the work-tool contact and improving the surface finish. Moreover, due to the eccentric cutting, a substantial gap exists between hole surface and tool. This helps chips comfortably evacuate for the cutting point without scratching/abrading the milled hole surface.

Figure 6(a) illustrates the impact cutting speed has on drilled surface roughness. Average surface roughness ($R_a=1.30\ \mu\text{m}$) was noted at a $25\ \text{m/min}$ lower speed. However, at $50\ \text{m/min}$, roughness was reduced to $1.13\ \mu\text{m}$. When a $75\ \text{m/min}$ speed was utilized, a surface roughness of $1.04\ \mu\text{m}$ was recorded. As noted, surface roughness reduces with cutting speed increase. With lower cutting speeds, continuous chips are formed during the drilling operation. The strained hardened chips entangle around the drill tool and scrape against the hole surface, resulting in deep grooves and scratches (see Fig. 7(a)). However, at higher cutting speed, surface roughness is reduced. At higher speed levels, the process stability increases due to the reduction in thrust force [36]. Also, higher speeds help break the chips, reducing the chip size and associated surface abrasion and roughness (see Fig. 7(b)).

Figure 6(b) illustrates the surface roughness behavior with cutting speed during helical milling. An average R_a of $0.41\ \mu\text{m}$ was noted in holes milled at $25\ \text{m/min}$. As cutting speed increased to $50\ \text{m/min}$, roughness increased to $0.55\ \mu\text{m}$. Surface roughness increased to $0.64\ \mu\text{m}$ when

Fig. 5 Surface roughness profile obtained from (a) Drilled hole, (b) Helical milled hole under similar productivity conditions



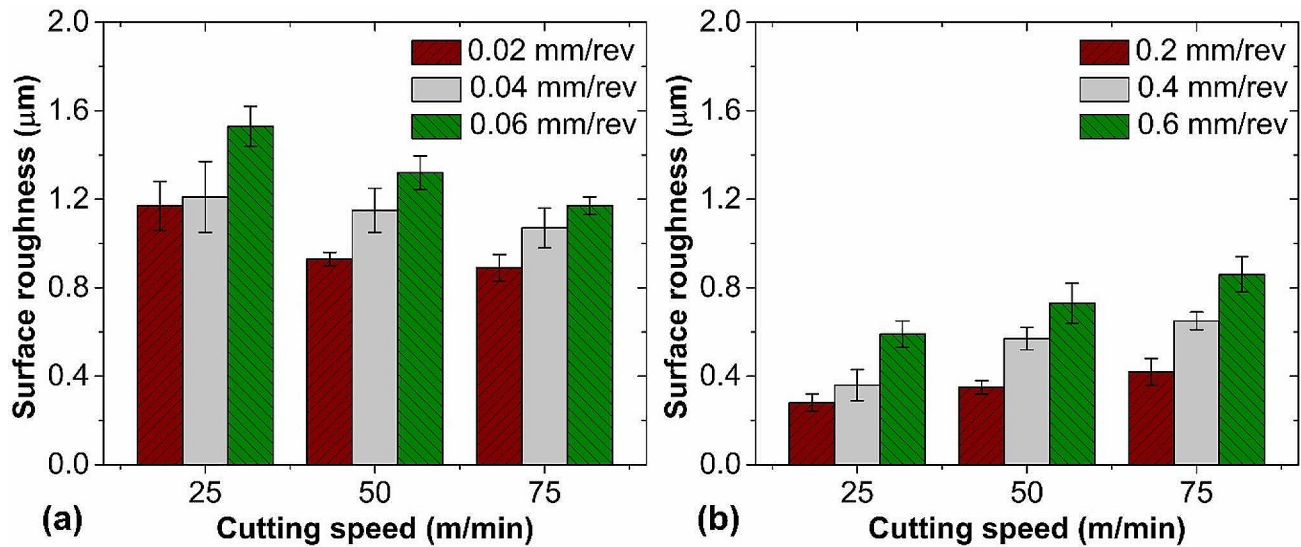


Fig. 6 Surface roughness against process variables for (a) Drilling (b) Helical milling

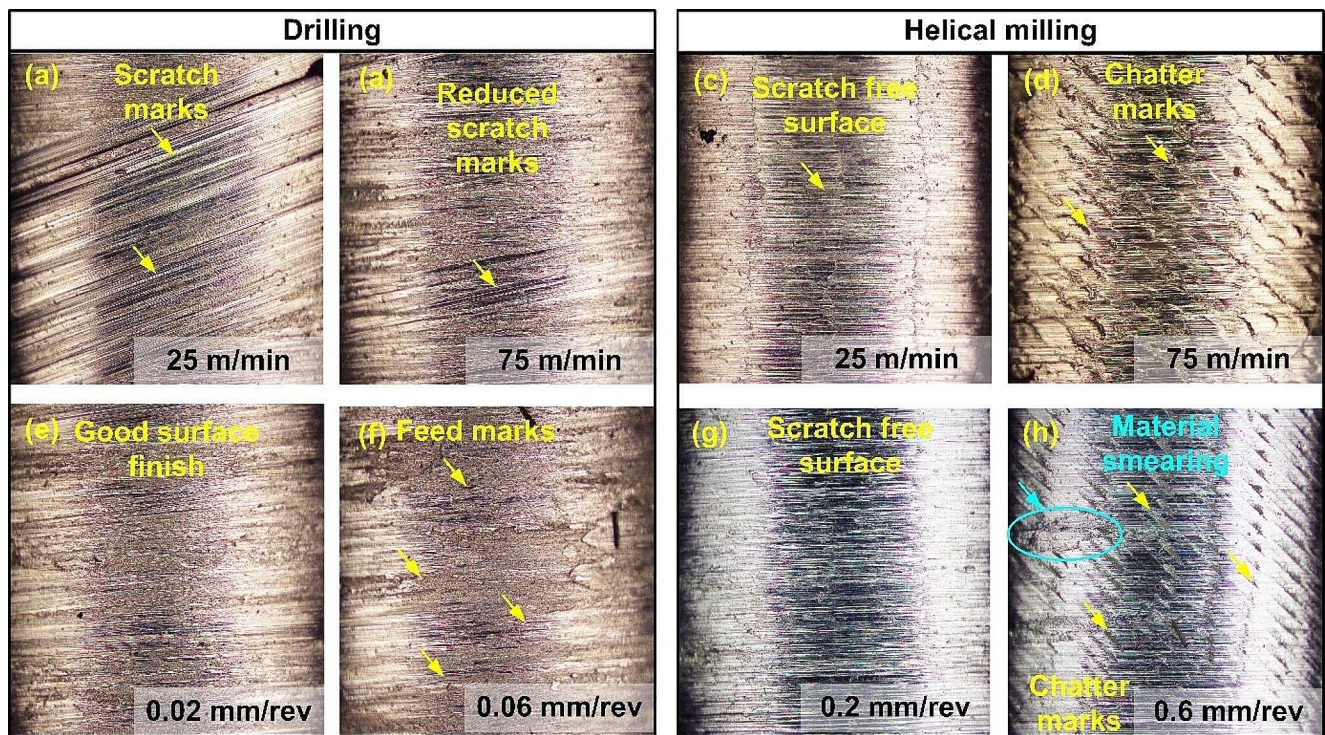


Fig. 7 Hole surface morphology during drilling and helical milling

cutting speed was 75 m/min. Surface roughness was lower at lower cutting speeds (see Fig. 7(c)) and increased drastically when a higher cutting speed was chosen. Higher surface roughness is attributed to tool-induced chatter (see Fig. 7(d)). At higher speeds, the thrust force increases. As a result, the slender end mill, which behaves like a cantilever beam, is subjected to bending load, creating machining instability and generating chatter marks on the hole surface [17].

Figure 6(a) also shows the influence of axial feed on the surface roughness during drilling operation. The maximum Ra of 0.99 µm was noted at a feed of 0.02 mm/rev. With the selection of a higher axial feed of 0.04 mm/rev, surface roughness increased to 1.14 µm, while the maximum roughness of 1.34 µm was recorded at 0.06 mm/rev. As indicated, surface roughness deteriorated as feed increased. Drilling at lower feed produced excellent surface-quality holes (see Fig. 7(e)). With higher axial feeds, feed marks on the hole

surface increased and became more prominent, as shown in Fig. 7(f). As a result, holes showcased poor surface finish [36].

Similarly, surface roughness increased as axial feed increased during helical milling. With a lower feed of 0.02 mm/rev, average roughness of 0.35 μm was obtained (see Fig. 6(b)). When the hole was machined with a higher axial feed of 0.04 mm/rev, the surface roughness increased to 0.53 μm . Maximum roughness of 0.72 μm was measured when a feed of 0.06 mm/rev was utilized. Lower surface roughness (see Fig. 7(g)) is attributed to lower cutting forces and discontinuous chip formation observed at lower axial feed [31]. However, with higher axial feeds, deterioration in the surface quality is attributed to chatter marks and chip adhesion. With higher feeds, contact length between tool-work increases, generating higher cutting forces. As a result, the end mill, due to its slenderness, undergoes deflection due to high loading conditions, resulting in unstable cutting [31] and increased surface roughness. Also, the smaller discontinuous chips produced during helical milling are extruded on the work surface. The chips get welded to the hole surface at higher temperatures, thus increasing the surface roughness (see Fig. 7(h)). Nevertheless, the helical milling process generated holes with better surface quality than drilling process.

3.3 Machining temperature

The temperature developed during the machining operations is critical as it influences the work surface characteristics and tool life. Therefore, machining temperature gathered during the machining trials was analyzed. Figure 8 shows the temperature cartographies obtained for the selected operations with similar machining conditions (Case 9).

During the drilling operation, machining temperature of 574.5 $^{\circ}\text{C}$ was recorded, while a temperature of 295.2 $^{\circ}\text{C}$ was registered during helical milling. Again, a 48.6% reduction

in the machining temperature can be observed when helical milling is employed. The higher temperature during drilling is ascribed to the machining kinematics and interface friction. In drilling, continuous contact prevails between workpiece-tool and tool-chip. This results in frictional heat. Besides, the poor thermal conductivity of Ti6Al4V hinders heat dissipation, thus contributing to temperature rise. However, helical milling exhibits lower machining temperatures. The lower magnitudes are attributed to intermittent nature of cutting in helical milling. Also, the generation of smaller discontinuous chips during the machining operation reduces interface friction and helps carry away the heat [31].

Furthermore, the influence of process variables on machining temperature was evaluated for both processes. The increasing evolution of cutting temperature with cutting speed for drilling can be verified in Fig. 9(a). Drilling with a 25 m/min cutting speed resulted in an average machining temperature of 357.6 $^{\circ}\text{C}$. A machining temperature of 420.5 $^{\circ}\text{C}$ was recorded at 50 m/min, and temperature rose to 525.4 $^{\circ}\text{C}$ when a 75 m/min cutting speed was employed. Temperature increased with the selection of higher levels of cutting speed. The rate of plastic deformation increases with the cutting speed, increasing the heat generated at the shear zone. Moreover, a substantial portion of heat is retained due to the inability of the material to dissipate heat at a faster rate owing to its poor thermal conductivity, thus increasing the machining temperature [17]. In addition, during drilling, continuous contact exists at the tool and workpiece interface. Resulting friction increases the heat generated and, thus, the machining temperature. A similar observation was made during the helical milling process, as evidenced by Fig. 9(b). Nevertheless, the temperature was significantly lower than that of the drilling process. In helical metal cutting occurs intermittently and produces discontinuous chips. Generated chips thus lower the frictional heat component and heat build-up, maintaining a lower temperature. Average machining temperature of 162.6 $^{\circ}\text{C}$ was recorded when

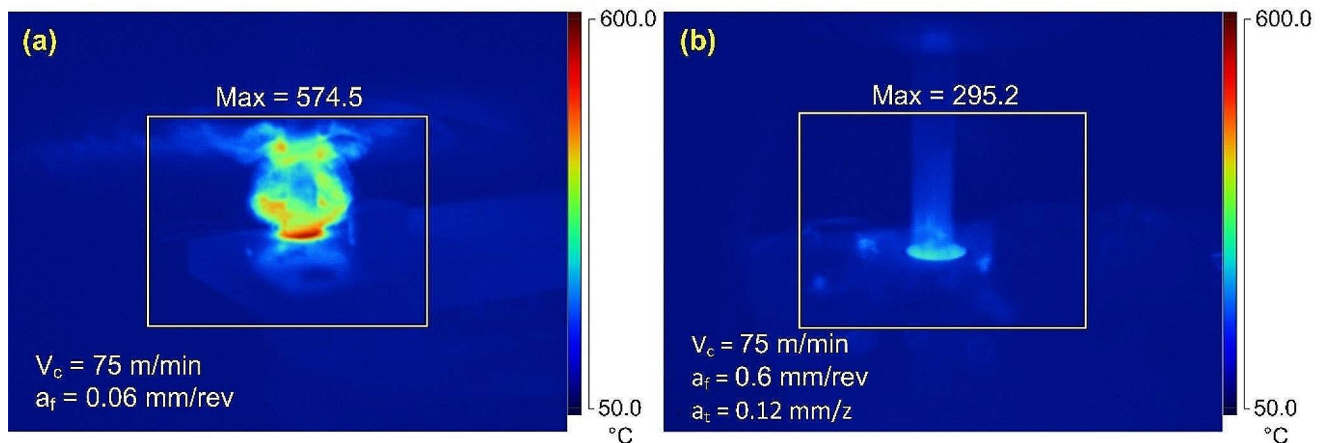


Fig. 8 Cartographies of machining temperature obtained for (a) Drilling (b) Helical milling

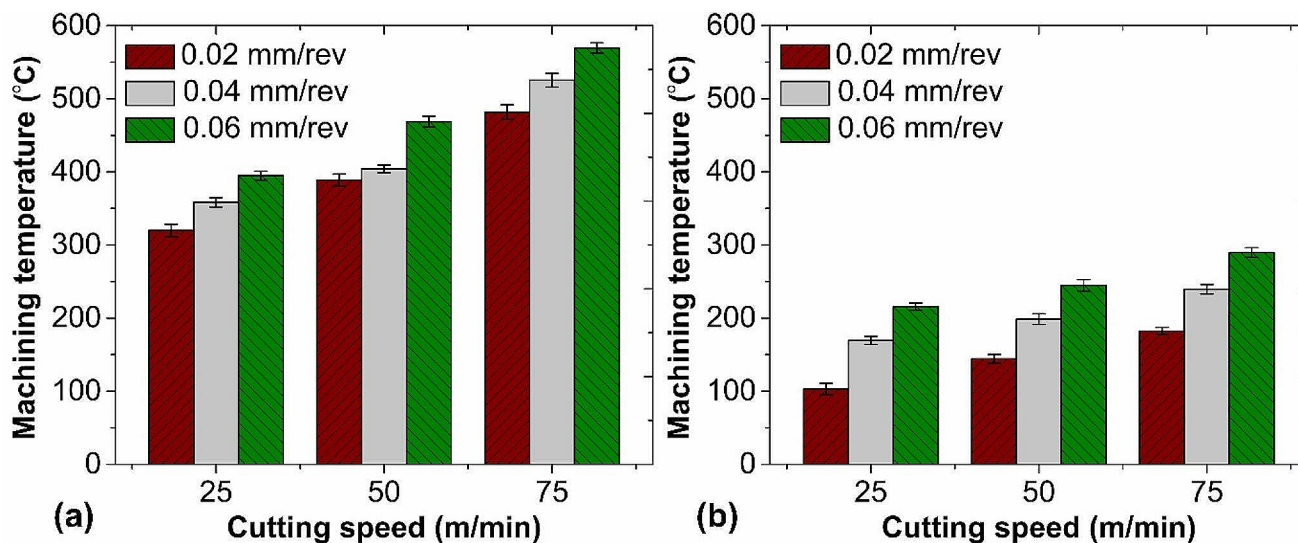


Fig. 9 Machining temperature against process variables for (a) Drilling (b) Helical milling

the cutting speed was 25 m/min. Temperature increased to 195.9 °C at 50 m/min. Highest temperature of 237.1 °C was witnessed at a speed of 75 m/min.

The selected axial feed also influenced the magnitude of machining temperature. Machining temperature increased as axial feed value increased from 0.02 to 0.06 mm/rev, as shown in Fig. 9(a). Drilling with a feed of 0.02 mm/rev, average temperature of 396.8 °C was recorded. The temperature increased to 429.2 °C when feed level was set at 0.04 mm/rev. Further increase in axial feed (0.06 mm/rev), machining temperature increased to 477.6 °C. Similarly, machining temperature increased during helical milling. Temperature increased from 143.1 °C (0.2 mm/rev) to 202.5 °C (0.4 mm/rev) and then reached 250 °C when feed of 0.6 mm/rev was utilized (see Fig. 9(b)). As axial feed increases, tool-workpiece contact increases. This increases the frictional load, and work-tool contact, thereby producing more heat and elevating the machining temperature.

3.4 Microhardness

The high strains and heat developed due to the machining-induced plastic deformation can severely affect the microhardness. Therefore, the subsurface microhardness was measured for the holes produced by the two operations. Figure 10(a) presents the evolution of microhardness with subsurface depth in conventionally drilled holes.

The measured microhardness near the hole surface (30 μm) was lower (340–380 HV) very close to the edge of the drilled holes and increased to attain higher values at depths away from the drilled hole surface. Lower microhardness close to the hole edge is attributed to material thermal softening. Severe plastic deformation while drilling Ti6Al4V alloy results in enormous heat generation and very

high temperatures. However, considering the low thermal conductivity, heat is accumulated at the edge of the hole. This gives rise to a thermally soft heat-affected zone (HAZ) having lower microhardness [25]. Further away from the drilled hole surface (depth greater than 90 μm), the surface microhardness rose to higher values (360–412 HV). During drilling, at depths away from the free surface, material exhibits dominant material deformation due to strain hardening. This results in the formation of machining-affected zone (MAZ), where alterations in microstructure take place. As a result, a significant increase in microhardness was recorded [25]. Moreover, further along the subsurface (500–650 μm), magnitude decreased to bulk hardness value, indicating an end to the influence of mechanical strain and heat on microhardness. A similar microhardness trend was witnessed for all the drilled holes. The microhardness magnitude varied with the selected levels of process variables. Figure 10(b) displays the variation in maximum microhardness with cutting speed. Even though machining temperature increased with cutting speed, associated thermal softening had little effect on the microhardness. On the contrary, maximum microhardness increased with cutting speed. The increase is attributed to MAZ formation. In the MAZ, material undergoes strain hardening and microstructure alteration. Moreover, the strain rates and amount of strain hardening increase with the rise in cutting speed from 25 m/min to 75 m/min, thereby increasing the microhardness.

Figure 10(b) also displays the maximum microhardness data with the axial feed. With the increase in axial feed, a temperature reduction and strain rate increase are noted. As a result, material hardening takes place, thus increasing the microhardness value. The maximum observed microhardness was 20% higher than bulk material hardness and was recorded in holes drilled at 75 m/min and 0.06 mm/rev axial

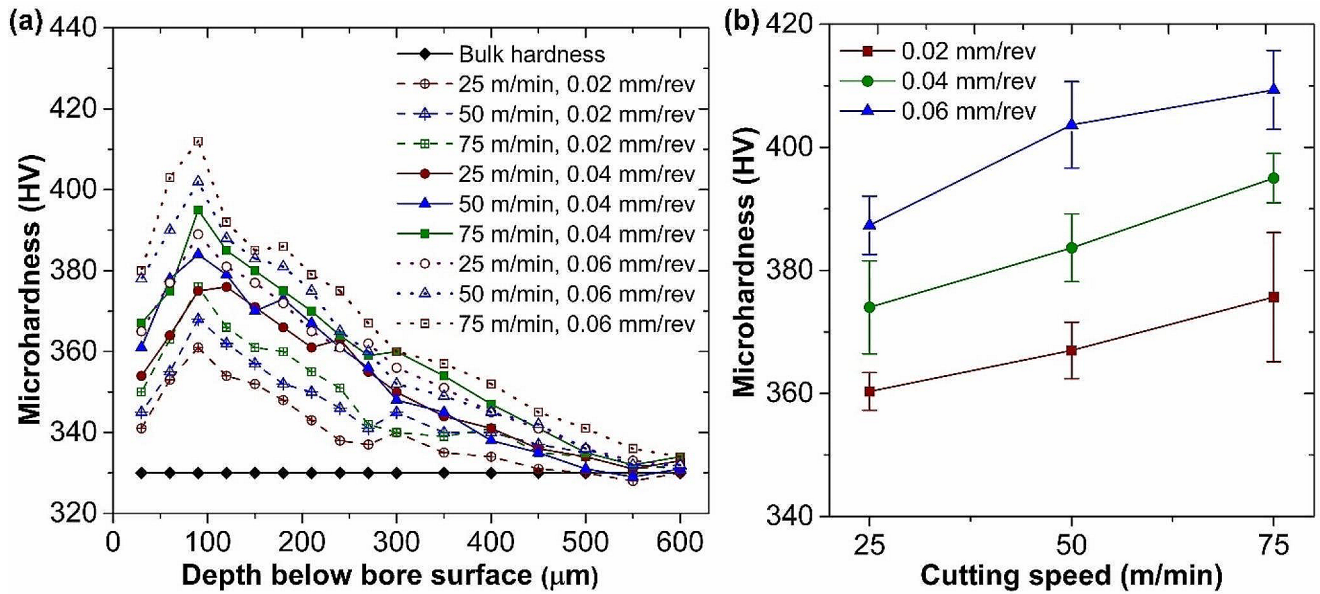


Fig. 10 (a) Microhardness profiles of holes drilled with different combinations of process variables. (b) Process variable influence on maximum microhardness during drilling

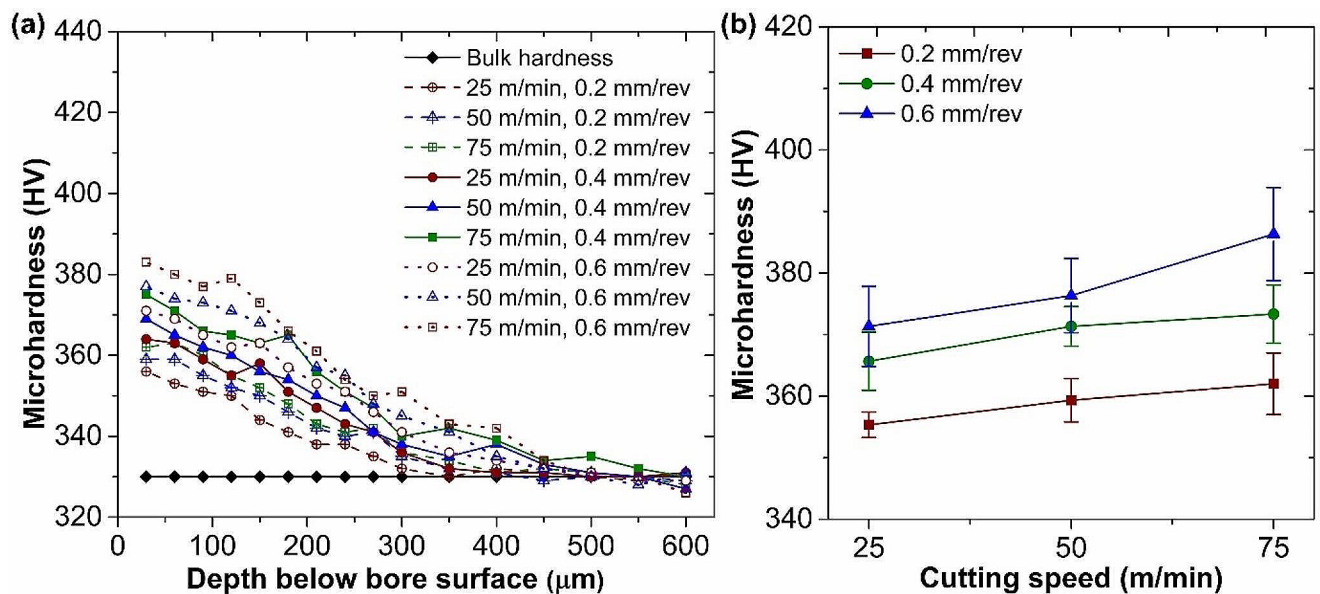


Fig. 11 (a) Microhardness profiles of holes milled with different combinations of process variables. (b) Process variable influence on maximum microhardness in helical milling

feed. Increase in microhardness is attributed to the increased strain rate at higher axial feed.

Figure 11(a) displays the evolution of microhardness in helically milled holes. Higher microhardness (356–383 HV) at a 30 μm sub-surface depth was recorded compared to bulk hardness. In helical milling, machining temperatures are considerably lower than drilling. Due to lower temperatures, the formation of HAZ is limited. Material dominantly exhibits strain hardening, which results in MAZ. The alterations in microstructure alteration in the MAZ increase the

microhardness very close to the edge of the milled holes. Additionally, helical milling is an intermittent cutting process. Heat accumulation occurs as the tool engages with the workpiece, while workpiece cooling commences as the tool exits the workpiece. Consequently, accumulation of internal work hardening takes place, thus increasing the microhardness. Therefore, microhardness measured near the machined surface is higher than bulk hardness. However, the microhardness decreases and equals the bulk microhardness as a

distance approaches 400–550 μm from free surface due to the neutralization of strain-rate hardening effect.

Figure 11(b) reveals the impact of cutting speed on microhardness during helical milling. Microhardness magnitude increased with cutting speed. The increase is attributed to the deformation-induced strain hardening. Also, the microhardness increased with the axial feed. Increase in material microhardness stems from the strain-hardening incurred due to mechanical deformation. For helical milling, maximum microhardness was 16% higher than the bulk hardness, and it was recorded while milling holes with a speed and feed combination of 75 m/min and 0.6 mm/rev. Results show that the maximum microhardness measured in drilled holes was considerably higher than in milled holes. Also, in conventional drilling, higher machining temperatures maintained the microhardness close to the bulk value near the subsurface (30 μm), while the effect of thermal softening was negligible in helical milling process.

3.5 Tool wear

The cutting tools were evaluated for changes in the profile after the conduction of experiments. Figure 12(a, b) displays the primary and secondary cutting edges of the drill, indicating material adhesion. Similarly, the end mill used for helical milling indicated the presence of adhered material, as seen in Fig. 12(c). Occurrence of material adhesion is well-established while machining Ti6Al4V alloy. Material adhesion is ascribed to the high chemical affinity exhibited by the work material towards the tool material and higher pressure generated during the machining process [37, 38]. During the machining operation, the work material will be subjected to very high contact pressure and close contact with the tool. Under such high pressure, the chemically active Ti6Al4V adheres to the tool surface. Moreover, due to low thermal conductivity, heat generated during plastic deformation accumulates at the cutting zone. With the rise in cutting temperature, chemical reactivity of Ti6Al4V alloy increases. The plastically deformed Ti6Al4V material adheres to the

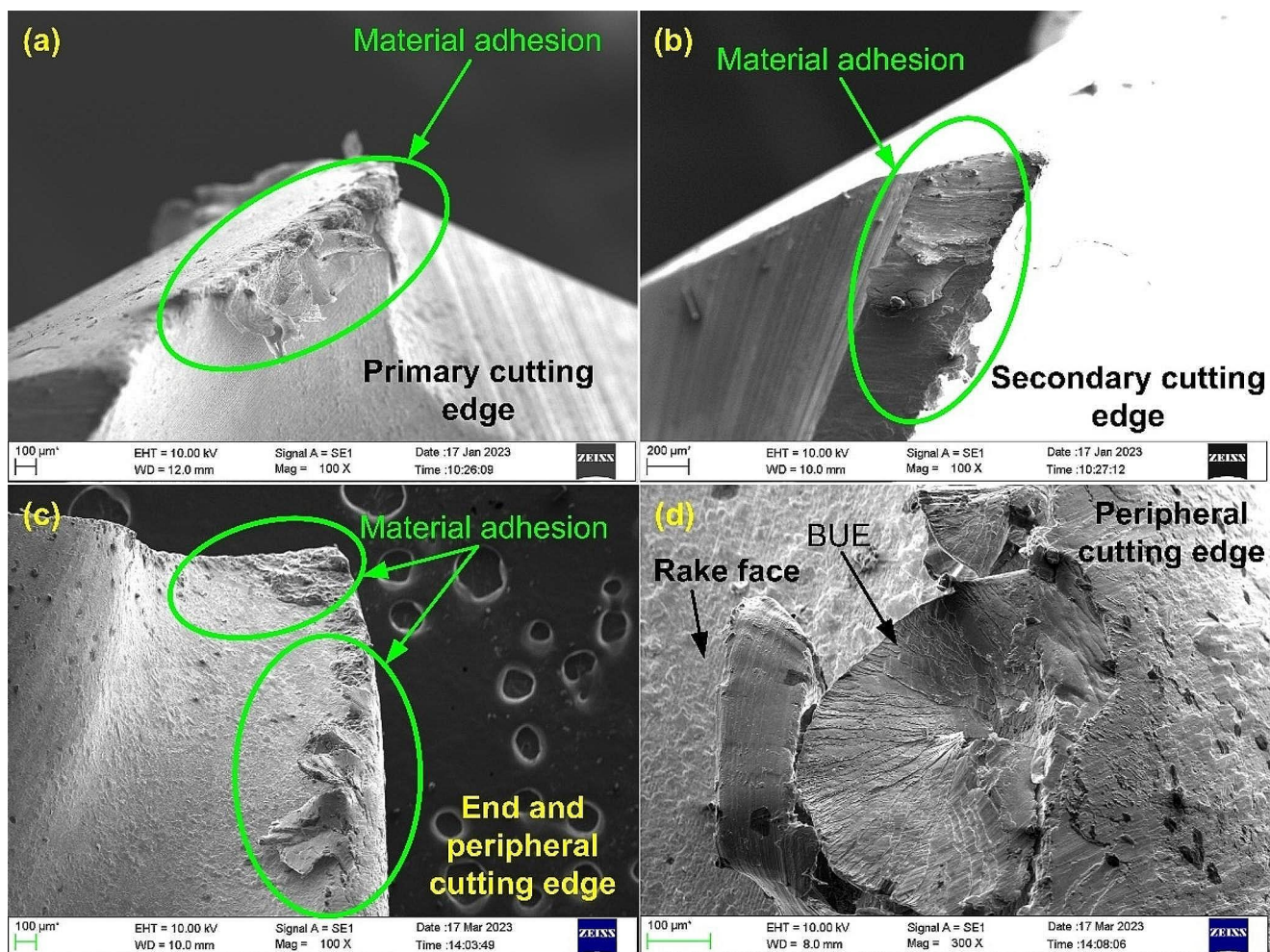


Fig. 12 Cutting tools showing material adhesion

tool material at such high cutting temperatures. The EDX analysis verifies the existence of adhered material at the cutting edges of the tools, as shown in Fig. 13.

In addition, the end mill showed signs of built-up edge (BUE) at the peripheral cutting edges, as seen in Fig. 12(d). During helical milling, peripheral cutting edges continually contact the workpiece. Moreover, under higher feed conditions, length of work-tool contact increases. The increased deformation increases the temperature and plasticizes the work material. Consequently, the material adheres to the cutting tool. Over a period of time, built-up edge (BUE) is formed due to the accumulation of the work material on the tool edges.

Furthermore, chisel edge and major flank face of the drill and end cutting edge and primary relief land on the end mill showed signs of material adhesion, as shown in Fig. 14(a, b). Adhered material can shield the cutting tool from accelerated wear. However, with extended machining, the adherend can become unstable and carried away by the flowing chips. During the process, the pull-out of tool material may occur, resulting in tool material loss and severe wear. Since a very limited number of holes were processed using the cutting tools, no severe tool wear was observed during helical milling and drilling operations.

3.6 Chip morphology

The size of the machined chips significantly affects the machining forces, surface quality, and tool life [26, 39]. Therefore, the chip morphology was analyzed considering both the hole-making operations. Long continuous chips were produced during the drilling operation, as seen in Fig. 15. The chip can be divided into four segments, namely, (a) initial spiral cone, (b) steady-state spiral cone, (c) transition between spiral cone and folded long ribbon, and (d) folded long ribbon [26]. As the drill enters the workpiece, initial spiral cone is produced. Steady-state spiral cone shape is produced once full penetration of tool takes place. However, as drill penetrates, resistance to chip ejection also increases. As a result, the chip morphology changes from spiral cone to folded ribbon. During conventional drilling, broken chips are desirable as they can easily move through the drill flutes and prevent any entanglement around the body of the drill. Therefore, influence of process variables on chip breakability was investigated.

Figure 16 reveals the impact of process variables on drilled chip morphology. As seen, axial feed influenced the chip size and shape. As feed was raised from 0.02 mm/rev to 0.06 mm/rev, a considerable reduction in the chip

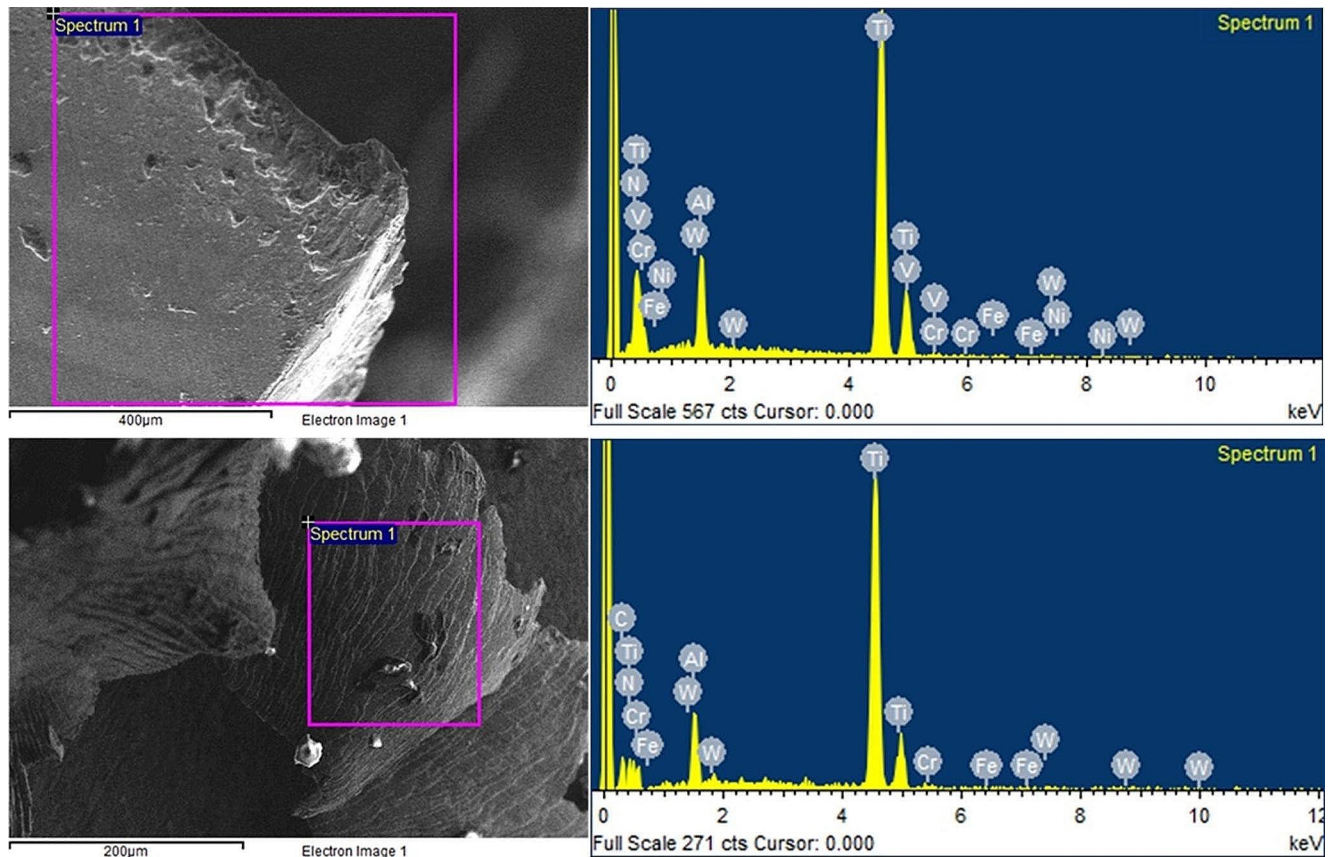


Fig. 13 EDX data indicating material adhesion

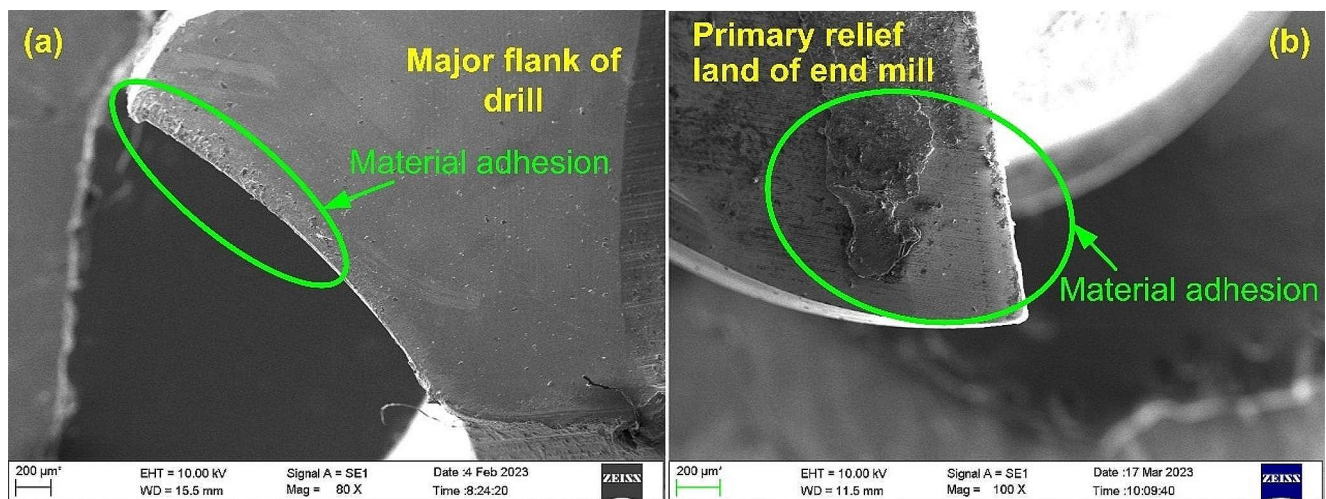
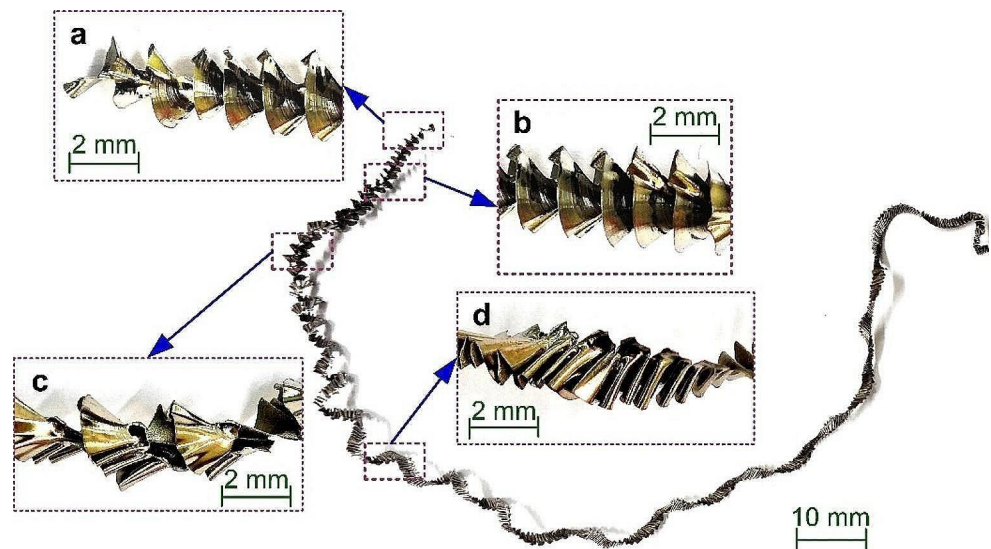


Fig. 14 Material adhesion at the (a) Drill front flank face, (b) Mill primary relief land

Fig. 15 Long continuous chip of Ti6Al4V alloy after dry drilling



length was noted. At higher feeds, chip cross-sectional area increases. This increases the chip stiffness and improves the chip breakability [26, 40]. Figure 15 also shows the change in chip size with drilling speed. A reduction in chip size was noted when speed increased from 25 m/min to 75 m/min. At higher cutting speeds, the kinetic energy increases. As a result, the chips wind up and undergo breakage [26, 41]. However, the impact cutting speed has on chip morphology is smaller in comparison to the axial feed. Overall, an axial feed of 0.06 mm/rev and a 75 m/min cutting speed are favorable for obtaining well-broken chips.

Helical milling generated well-broken, extremely small discontinuous chips. Figure 17 displays the variation in the morphology during helical milling. Powdery chips were developed at lower axial feed (0.2 mm/rev). In contrast, larger lamellar chips were observed at a 0.6 mm/rev feed. As indicated, the size of the chips increased with the feed

value. The increase in size is attributed to increase in uncut chip thickness. Size also increased with the cutting speed. Smaller chips were noticed at a lower speed of 25 m/min. However, larger but broken chips were noted at a higher speed of 75 m/min. In helical milling, machining temperature increases with cutting speed. The subsequent increase in material ductility reduces the possibility of chip breakage, producing ribbon-like chips. However, chips produced during helical milling were well broken, which is very desirable while machining Ti6Al4V alloy.

4 Conclusions

The work systematically investigated the drilling and helical milling of Ti6Al4V alloy using sustainable dry conditions. The two operations were appraised considering the

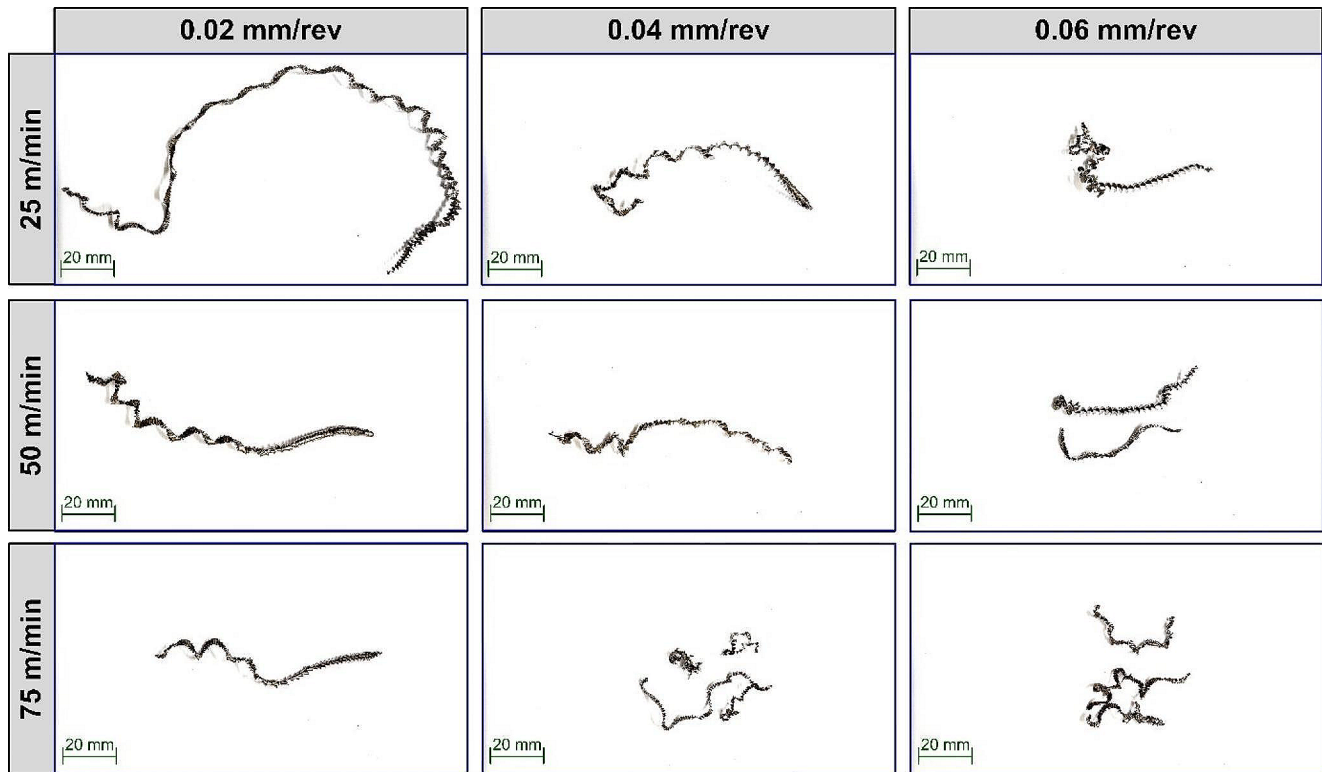


Fig. 16 Drilled chip morphology variation with cutting speed and axial feed

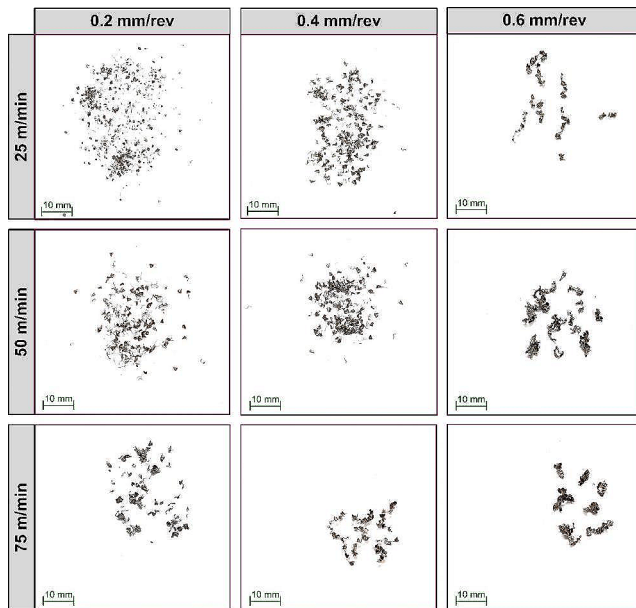


Fig. 17 Chip morphology variation with cutting speed and axial feed during dry helical milling

chip morphology, microhardness, machining temperature, surface roughness, and tool wear. The conclusions drawn are listed:

- The employment of helical milling helped lower the thrust force magnitude by 72–75% compared to drilling process, even during dry cutting. The difference in the thrust force is attributed to the machining kinematics associated with the two processes. Moreover, thrust force decreased as cutting speed increased, while an upward trend was ascertained with axial feed for both hole-making operations.
- Helical milling is capable of producing surface finish superior to conventional drilling operations. The surface roughness reduced by 27–76% with the incorporation of helical milling process. Drilled holes displayed the presence of scratch marks formed due to the abrasion between the work material and long continuous chips. Chatter marks were observed in holes helically milled at higher speeds and feed conditions.
- The machining temperature was significantly lower during helical milling. With the employment of helical milling, temperature lowered by 49–68% as compared to drilling operations. The lower temperature helped in preventing any thermal damage to the work material.

The magnitude of machining increased as cutting speed and axial feed increased for the operations.

- The microhardness behavior of the work material post-machining is different from the employment of the two hole-making operations. The subsurface microhardness in drilled holes was lower due to the thermal softening mechanism taking precedence over the strain-hardening behavior exhibited by the material. Meanwhile, helical milled holes exhibited higher microhardness near the subsurface as a result of strain hardening behavior exhibited by the material. Moreover, microhardness increased as speed and feed increased for the selected operations.
- Dry machining of Ti6Al4V alloy transpired in material adhesion at the primary and secondary cutting edges. Material adhesion was severe during helical milling, resulting in built-up edge formation.
- Long continuous chips were produced during drilling, while helical milling generated discontinuous powdery chips. Cutting speed and axial feed impacted the chip morphology. Chip size reduced with the increase in axial feed and cutting speed. However, the influence of axial feed on chip breakability was significantly higher than that of cutting speed. In general, selection of helical milling was beneficial as it generated well-broken chips.

Funding Open access funding provided by Manipal Academy of Higher Education, Manipal

Declarations

Competing interests The authors declare no competing interests.

Open Access This article is licensed under a Creative Commons Attribution 4.0 International License, which permits use, sharing, adaptation, distribution and reproduction in any medium or format, as long as you give appropriate credit to the original author(s) and the source, provide a link to the Creative Commons licence, and indicate if changes were made. The images or other third party material in this article are included in the article's Creative Commons licence, unless indicated otherwise in a credit line to the material. If material is not included in the article's Creative Commons licence and your intended use is not permitted by statutory regulation or exceeds the permitted use, you will need to obtain permission directly from the copyright holder. To view a copy of this licence, visit <http://creativecommons.org/licenses/by/4.0/>.

References

- Zang, M.C., Niu, H.Z., Zhang, H.R., Tan, H., Zhang, D.L.: Cryogenic tensile properties and deformation behavior of a superhigh strength metastable beta titanium alloy Ti–15Mo–2Al. *Mater. Sci. Eng. A*. **817**, 141344 (2021). <https://doi.org/10.1016/j.msea.2021.141344>
- Cai, C., Gao, X., Teng, Q., Kiran, R., Liu, J., Wei, Q., Shi, Y.: Hot isostatic pressing of a near α -Ti alloy: Temperature optimization, microstructural evolution and mechanical performance evaluation. *Mater. Sci. Eng. A*. **802**, 140426 (2021). <https://doi.org/10.1016/j.msea.2020.140426>
- Zhang, X., Liu, S., Liu, Y., Guo, H., Shi, W.: Titanium Alloy fabricated by Additive Manufacturing for Medical Applications: Obtaining, characterization and application—review. *Met. (Basel)*. **13**, 462 (2023). <https://doi.org/10.3390/met13030462>
- Nyamekye, P., Golroudbary, S.R., Piili, H., Luukka, P., Kraslawski, A.: Impact of additive manufacturing on titanium supply chain: Case of titanium alloys in automotive and aerospace industries. *Adv. Ind. Manuf. Eng.* **6**, 100112 (2023)
- Nyamekye, P., Rahimpour Golroudbary, S., Piili, H., Luukka, P., Kraslawski, A.: Impact of additive manufacturing on titanium supply chain: Case of titanium alloys in automotive and aerospace industries. *Adv. Ind. Manuf. Eng.* **6**, 100112 (2023). <https://doi.org/10.1016/j.aime.2023.100112>
- Zhou, M., Hu, T., Mu, X., Zhao, M., JianweiYang, Ye, Q., Xu, P., Yang, L., Xin, F.: Significant step towards efficient electrical discharge machining titanium alloys. *Int. J. Adv. Manuf. Technol.* **127**, 3905–3918 (2023). <https://doi.org/10.1007/s00170-023-11767-6>
- Palanikumar, S.R., Boppana, K., Natarajan, S.B.: Analysis of chip formation and Temperature Measurement in Machining of Titanium Alloy (Ti-6Al-4V). *Exp. Tech.* **47**, 517–529 (2023). <https://doi.org/10.1007/s40799-021-00537-2>
- Matuszak, J., Zaleski, K., Zyśko, A.: Investigation of the impact of high-speed machining in the milling process of Titanium Alloy on Tool wear, Surface Layer properties, and fatigue life of the machined object. *Mater. (Basel)*. **16**, 5361 (2023). <https://doi.org/10.3390/ma16155361>
- Tascioglu, E., Gharibi, A., Kaynak, Y.: High speed machining of near-beta titanium Ti-5553 alloy under various cooling and lubrication conditions. *Int. J. Adv. Manuf. Technol.* **102**, 4257–4271 (2019). <https://doi.org/10.1007/s00170-019-03291-3>
- Gupta, M.K., Song, Q., Liu, Z., Sarikaya, M., Mia, M., Jamil, M., Singla, A.K., Bansal, A., Pimenov, D.Y., Kuntoğlu, M.: Tribological performance based machinability investigations in cryogenic cooling assisted turning of α - β titanium Alloy. *Tribol Int.* **160**, 107032 (2021). <https://doi.org/10.1016/j.triboint.2021.107032>
- Chen, G., Caudill, J., Chen, S., Jawahir, I.S.: Machining-induced surface integrity in titanium alloy Ti-6Al-4V: An investigation of cutting edge radius and cooling/lubricating strategies. *J. Manuf. Process.* **74**, 353–364 (2022). <https://doi.org/10.1016/j.jmapro.2021.12.016>
- García-Martínez, E., Miguel, V., Martínez-Martínez, A., Manjabacas, M.C., Coello, J.: Sustainable lubrication methods for the machining of Titanium alloys: An overview. *Mater. (Basel)*. **12**, 3852 (2019). <https://doi.org/10.3390/ma12233852>
- Gajrani, K.K., Sankar, M.R.: Role of eco-friendly cutting fluids and cooling techniques in machining. In: Gupta, K. (ed.) *Materials Forming, Machining and Post Processing, Materials Forming, Machining and Tribology*, pp. 159–181. Springer, Cham (2020). https://doi.org/10.1007/978-3-030-18854-2_7
- Khanna, N., Shah, P., Sarikaya, M., Pusavec, F.: Energy consumption and ecological analysis of sustainable and conventional cutting fluid strategies in machining 15–5 PHSS. *Sustain. Mater. Technol.* **32**, e00416 (2022). <https://doi.org/10.1016/j.susmat.2022.e00416>
- Yuan, C.G., Pramanik, A., Basak, A.K., Prakash, C., Shankar, S.: Drilling of titanium alloy (Ti6Al4V) – a review. *Mach. Sci. Technol.* **25**, 637–702 (2021). <https://doi.org/10.1080/10910344.2021.1925295>
- Aamir, M., Giasin, K., Tolouei-Rad, M., Vafadar, A.: A review: Drilling performance and hole quality of aluminium alloys for aerospace applications. *J. Mater. Res. Technol.* **9**, 12484–12500 (2020). <https://doi.org/10.1016/j.jmrt.2020.09.003>

17. Akula, S., Nayak, S.N., Bolar, G., Managuli, V.: Comparison of conventional drilling and helical milling for hole making in Ti6Al4V titanium alloy under sustainable dry condition. *Manuf. Rev.* **8**, 12 (2021). <https://doi.org/10.1051/mfreview/2021010>
18. Kumar, A., Bhardwaj, R., Joshi, S.S.: Thermal modeling of drilling process in titanium alloy (Ti-6Al-4V). *Mach. Sci. Technol.* **24**, 341–365 (2020). <https://doi.org/10.1080/10910344.2019.1698607>
19. Coelho, W.A., Pereira, R.B.D., Lauro, C.H., Brandão, L.C., Davim, J.P.: Comparative study of deep drilling in the Ti-6Al-4 V ELI titanium alloy using standard and high-feed rate. *Int. J. Adv. Manuf. Technol.* **126**, 4157–4170 (2023). <https://doi.org/10.1007/s00170-023-11351-y>
20. Zhang, X., Peng, Z., Li, Z., Sui, H., Zhang, D.: Influences of machining parameters on tool performance when high-speed ultrasonic vibration cutting titanium alloys. *J. Manuf. Process.* **60**, 188–199 (2020). <https://doi.org/10.1016/j.jmapro.2020.10.053>
21. Li, R., Shih, A.J.: Tool temperature in titanium drilling. *J. Manuf. Sci. Eng.* **129**, 740–749 (2007). <https://doi.org/10.1115/1.2738120>
22. Le Coz, G., Marinescu, M., Devillez, A., Dudzinski, D., Velnom, L.: Measuring temperature of rotating cutting tools: Application to MQL drilling and dry milling of aerospace alloys. *Appl. Therm. Eng.* **36**, 434–441 (2012). <https://doi.org/10.1016/j.applthermaleng.2011.10.060>
23. Singh, M., Dhiman, S., Singh, H., Berndt, C.C.: Optimization of modulation-assisted drilling of Ti-6Al-4V aerospace alloy via response surface method. *Mater. Manuf. Process.* **35**, 1313–1329 (2020). <https://doi.org/10.1080/10426914.2020.1772487>
24. Zhu, Z., Sui, S., Sun, J., Li, J., Li, Y.: Investigation on performance characteristics in drilling of Ti6Al4V alloy. *Int. J. Adv. Manuf. Technol.* **93**, 651–660 (2017). <https://doi.org/10.1007/s00170-017-0508-6>
25. Varote, N., Joshi, S.S.: Microstructural Analysis of Machined Surface Integrity in Drilling a Titanium Alloy. *J. Mater. Eng. Perform.* **26**, 4391–4401 (2017). <https://doi.org/10.1007/s11665-017-2864-7>
26. Zhu, Z., Guo, K., Sun, J., Li, J., Liu, Y., Chen, L., Zheng, Y.: Evolution of 3D chip morphology and phase transformation in dry drilling Ti6Al4V alloys. *J. Manuf. Process.* **34**, 531–539 (2018). <https://doi.org/10.1016/j.jmapro.2018.07.001>
27. Pereira, R.B.D., Brandão, L.C., de Paiva, A.P., Ferreira, J.R., Davim, J.P.: A review of helical milling process. *Int. J. Mach. Tools Manuf.* **120**, 27–48 (2017). <https://doi.org/10.1016/j.ijmachtools.2017.05.002>
28. Festas, A.J., Pereira, R.B., Ramos, A., Davim, J.P.: A study of the effect of conventional drilling and helical milling in surface quality in titanium Ti-6Al-4V and Ti-6Al-7Nb alloys for medical applications. *Arab. J. Sci. Eng.* **46**, 2361–2369 (2021)
29. Wang, B., Chang, K., Wang, M., Zhang, F., Zhang, Y., Zheng, Y.: Experimental studies on helical milling process to improve hole quality for the Superalloy (MSRR7197). *Int. J. Adv. Manuf. Technol.* **99**, 1449–1458 (2018). <https://doi.org/10.1007/s00170-018-2588-3>
30. Iqbal, A., Suhaimi, H., Zhao, W., Jamil, M., Nauman, M.M., He, N., Zaini, J.: Sustainable milling of Ti-6Al-4V: Investigating the effects of Milling Orientation, Cutter's Helix Angle, and type of Cryogenic Coolant. *Metals*. **10**, 258 (2020). <https://doi.org/10.3390/met10020258>
31. Shanmugam, R., Baloor, S.S., Koklu, U., Polishetty, A., Bolar, G.: Machining temperature, Surface Integrity and Burr Size Investigation during coolant-free hole milling in Ti6Al4V Titanium Alloy. *Lubricants*. **11**, 349 (2023). <https://doi.org/10.3390/lubricants11080349>
32. Geng, D., Sun, Z., Liu, Y., Liu, L., Ying, E., Cai, J., et al.: Unravelling the influence of vibration on material removal and microstructure evolution in ultrasonic transversal vibration-assisted helical milling of Ti-6Al-4V holes. *J. Mater. Proc. Technol.* **326**, 118320 (2024). <https://doi.org/10.1016/j.jmatprotec.2024.118320>
33. Cantero, J.L., Tardio, M.M., Canteli, J.A., Marcos, M., Miguélez, M.H.: Dry drilling of alloy Ti-6Al-4V. *Int. J. Mach. Tool. Manuf.* **45**(11), 1246–1255 (2005). <https://doi.org/10.1016/j.ijmachtools.2005.01.010>
34. Wu, J., Han, R.D.: Friction characteristics in green drilling titanium alloy Ti6Al4V. *J. Shanghai Jiaotong Uni (Sci)*. **17**, 684–689 (2012). <https://doi.org/10.1007/s12204-012-1346-1>
35. Kumar, Y., Singh, H.: Multi-response optimization in dry turning process using Taguchi's approach and utility concept. *Proc. Mater. Sci.* **5**, 2142–2151 (2014). <https://doi.org/10.1016/j.mspro.2014.07.417>
36. Iyer, R., Koshy, P., Ng, E.: Helical milling: An enabling technology for hard machining precision holes in AISI D2 tool steel. *Int. J. Mach. Tools Manuf.* **47**, 205–210 (2007). <https://doi.org/10.1016/j.ijmachtools.2006.04.006>
37. Batista Ponce, M., Vazquez-Martinez, J.M., Davim, J.P., Salguero Gomez, J.: Analysis of secondary adhesion wear mechanism on hard machining of titanium aerospace alloy. *Materials*. **12**(12), 2015 (2019). <https://doi.org/10.3390/ma12122015>
38. Li, C., Chen, J., Li, S., Xu, M., Liu, X., Wei, R., et al.: Study of chip adhesion behavior in titanium alloy dry milling process based on image extraction technology. *Int. J. Adv. Manuf. Technol.* **126**(5), 2633–2645 (2023). <https://doi.org/10.1007/s00170-023-11249-9>
39. Usca, Ü.A., Uzun, M., Sap, S., Giasin, K., Pimenov, D.Y., Prakash, C.: Determination of machinability metrics of AISI 5140 steel for gear manufacturing using different cooling/lubrication conditions. *J. Mater. Res. Technol.* **21**, 893–904 (2022). <https://doi.org/10.1016/j.jmrt.2022.09.067>
40. Xu, J., Mansori, E.: Experimental study on drilling mechanisms and strategies of hybrid CFRP/Ti stacks. *Compos. Struct.* **157**, 461–482 (2016). <https://doi.org/10.1016/j.compstruct.2016.07.025>
41. Sridhar, A.K., Bolar, G., Padmaraj, N.H.: Comprehensive experimental investigation on drilling multi-material carbon fiber reinforced aluminum laminates. *J. King Saud Univ. - Eng. Sci.* **34**, 391–401 (2022). <https://doi.org/10.1016/j.jksues.2021.11.004>

Publisher's Note Springer Nature remains neutral with regard to jurisdictional claims in published maps and institutional affiliations.